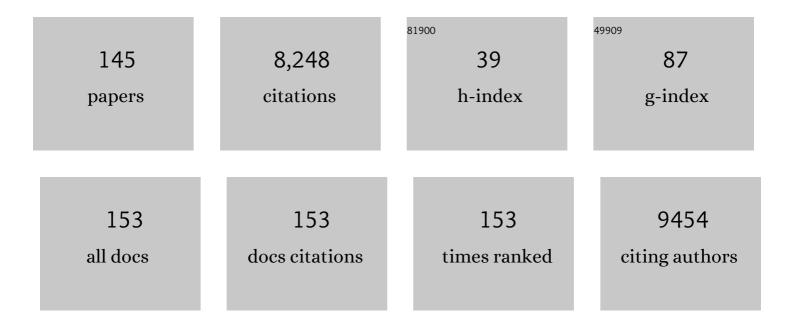
List of Publications by Year in descending order

Source: https://exaly.com/author-pdf/2080755/publications.pdf Version: 2024-02-01



DEAN E WONG

#	Article	IF	CITATIONS
1	Consensus Nomenclature for in vivo Imaging of Reversibly Binding Radioligands. Journal of Cerebral Blood Flow and Metabolism, 2007, 27, 1533-1539.	4.3	1,840
2	In Vivo Imaging of Amyloid Deposition in Alzheimer Disease Using the Radioligand ¹⁸ F-AV-45 (Flobetapir F 18). Journal of Nuclear Medicine, 2010, 51, 913-920.	5.0	607
3	Association Between Midlife Vascular Risk Factors and Estimated Brain Amyloid Deposition. JAMA - Journal of the American Medical Association, 2017, 317, 1443.	7.4	451
4	Self-reported Sleep and β-Amyloid Deposition in Community-Dwelling Older Adults. JAMA Neurology, 2013, 70, 1537-43.	9.0	414
5	Increased Occupancy of Dopamine Receptors in Human Striatum during Cue-Elicited Cocaine Craving. Neuropsychopharmacology, 2006, 31, 2716-2727.	5.4	280
6	Dopamine D2 and D3 Receptor Occupancy in Normal Humans Treated with the Antipsychotic Drug Aripiprazole (OPC 14597) A Study Using Positron Emission Tomography and [11C]Raclopride. Neuropsychopharmacology, 2002, 27, 248-259.	5.4	261
7	Mechanisms of Dopaminergic and Serotonergic Neurotransmission in Tourette Syndrome: Clues from an In Vivo Neurochemistry Study with PET. Neuropsychopharmacology, 2008, 33, 1239-1251.	5.4	227
8	Dopamine D2 receptor occupancy of lumateperone (ITI-007): a Positron Emission Tomography Study in patients with schizophrenia. Neuropsychopharmacology, 2019, 44, 598-605.	5.4	207
9	Mechanism of New Antipsychotic Medications. Archives of General Psychiatry, 2003, 60, 974.	12.3	200
10	Positron emission tomography imaging of serotonin transporters in the human brain using [11C](+)McN5652. Synapse, 1995, 20, 37-43.	1.2	161
11	The Role of Imaging in Proof of Concept for CNS Drug Discovery and Development. Neuropsychopharmacology, 2009, 34, 187-203.	5.4	161
12	Effects of endogenous dopamine on kinetics of [3H]N-methylspiperone and [3H]raclopride binding in the rat brain. Synapse, 1991, 9, 188-194.	1.2	126
13	The ARIC-PET amyloid imaging study. Neurology, 2016, 87, 473-480.	1.1	119
14	Arterial stiffness and dementia pathology. Neurology, 2018, 90, e1248-e1256.	1.1	114
15	Standardization of amyloid quantitation with florbetapir standardized uptake value ratios to the Centiloid scale. Alzheimer's and Dementia, 2018, 14, 1565-1571.	0.8	98
16	The Role of Dopamine in Value-Based Attentional Orienting. Current Biology, 2016, 26, 550-555.	3.9	96
17	¹⁸ F-FPEB, a PET Radiopharmaceutical for Quantifying Metabotropic Glutamate 5 Receptors: A First-in-Human Study of Radiochemical Safety, Biokinetics, and Radiation Dosimetry. Journal of Nuclear Medicine, 2013, 54, 388-396.	5.0	95
18	Localization of serotonin 5-HT2 receptors in living human brain by positron emission tomography using N1-([11C]-methyl)-2-BR-LSD. Synapse, 1987, 1, 393-398.	1.2	94

#	Article	IF	CITATIONS
19	In vivo imaging of dopamine reuptake sites in the primate brain using single photon emission computed tomography (SPECT) and iodine-123 labeled RTI-55. Synapse, 1992, 10, 169-172.	1.2	85
20	Characterization of 3 Novel Tau Radiopharmaceuticals, ¹¹ C-RO-963, ¹¹ C-RO-643, and ¹⁸ F-RO-948, in Healthy Controls and in Alzheimer Subjects. Journal of Nuclear Medicine, 2018, 59, 1869-1876.	5.0	81
21	Effects of amyloid pathology and neurodegeneration on cognitive change in cognitively normal adults. Brain, 2018, 141, 2475-2485.	7.6	78
22	Preclinical Evaluation of ¹⁸ F-RO6958948, ¹¹ C-RO6931643, and ¹¹ C-RO6924963 as Novel PET Radiotracers for Imaging Tau Aggregates in Alzheimer Disease. Journal of Nuclear Medicine, 2018, 59, 675-681.	5.0	71
23	Human Brain Imaging of α7 nAChR with [18F]ASEM: a New PET Radiotracer for Neuropsychiatry and Determination of Drug Occupancy. Molecular Imaging and Biology, 2014, 16, 730-738.	2.6	69
24	Specific Binding of [11C]Raclopride and N-[3H]Propyl-Norapomorphine to Dopamine Receptors in Living Mouse Striatum: Occupancy by Endogenous Dopamine and Guanosine Triphosphate–Free G Protein. Journal of Cerebral Blood Flow and Metabolism, 2002, 22, 596-604.	4.3	68
25	A multivariate nonlinear mixed effects model for longitudinal image analysis: Application to amyloid imaging. Neurolmage, 2016, 134, 658-670.	4.2	68
26	Evaluation of ¹⁸ F-RO-948 PET for Quantitative Assessment of Tau Accumulation in the Human Brain. Journal of Nuclear Medicine, 2018, 59, 1877-1884.	5.0	64
27	Individual estimates of age at detectable amyloid onset for risk factor assessment. Alzheimer's and Dementia, 2016, 12, 373-379.	0.8	63
28	Molecular imaging of serotonin degeneration in mild cognitive impairment. Neurobiology of Disease, 2017, 105, 33-41.	4.4	61
29	Changes in Aβ biomarkers and associations with APOE genotype in 2Âlongitudinal cohorts. Neurobiology of Aging, 2015, 36, 2333-2339.	3.1	60
30	Predicting the success of a radiopharmaceutical for in vivo imaging of central nervous system neuroreceptor systems. Molecular Imaging and Biology, 2003, 5, 350-362.	2.6	54
31	Excessive daytime sleepiness and napping in cognitively normal adults: associations with subsequent amyloid deposition measured by PiB PET. Sleep, 2018, 41, .	1.1	53
32	Reciprocal alterations in cortical cannabinoid receptor 1 binding relative to protein immunoreactivity and transcript levels in schizophrenia. Schizophrenia Research, 2014, 159, 124-129.	2.0	52
33	Doses of GBR12909 that suppress cocaine self-administration in non-human primates substantially occupy dopamine transporters as measured by [11C] WIN35,428 PET scans. , 1999, 32, 44-50.		50
34	GBR12909 attenuates amphetamine-induced striatal dopamine release as measured by [11C]raclopride continuous infusion PET scans. Synapse, 1999, 33, 268-273.	1.2	50
35	Cerebral Glucose Utilization in Polysubstance Abuse. Neuropsychopharmacology, 1995, 13, 21-31.	5.4	48
36	Development of a High-Affinity PET Radioligand for Imaging Cannabinoid Subtype 2 Receptor. Journal of Medicinal Chemistry, 2016, 59, 7840-7855.	6.4	47

3

#	Article	IF	CITATIONS
37	PET Imaging of High-Affinity α4β2 Nicotinic Acetylcholine Receptors in Humans with ¹⁸ F-AZAN, a Radioligand with Optimal Brain Kinetics. Journal of Nuclear Medicine, 2013, 54, 1308-1314.	5.0	46
38	Linking dopaminergic reward signals to the development of attentional bias: A positron emission tomographic study. NeuroImage, 2017, 157, 27-33.	4.2	46
39	Metabolic Syndrome and Amyloid Accumulation in the Aging Brain. Journal of Alzheimer's Disease, 2018, 65, 629-639.	2.6	44
40	Cerebral Glucose Utilization Is Reduced in Second Test Session. Journal of Cerebral Blood Flow and Metabolism, 1997, 17, 704-712.	4.3	43
41	GM1 ganglioside in Parkinson's disease: Pilot study of effects on dopamine transporter binding. Journal of the Neurological Sciences, 2015, 356, 118-123.	0.6	42
42	Objectively measured sleep and β-amyloid burden in older adults: A pilot study. SAGE Open Medicine, 2014, 2, 205031211454652.	1.8	41
43	Early affective changes and increased connectivity in preclinical Alzheimer's disease. Alzheimer's and Disease Monitoring, 2018, 10, 471-479.	2.4	40
44	Transcranial Recording of Electrophysiological Neural Activity in the Rodent Brain in vivo Using Functional Photoacoustic Imaging of Near-Infrared Voltage-Sensitive Dye. Frontiers in Neuroscience, 2019, 13, 579.	2.8	40
45	Listening to membrane potential: photoacoustic voltage-sensitive dye recording. Journal of Biomedical Optics, 2017, 22, 045006.	2.6	38
46	Bile acid synthesis, modulation, and dementia: A metabolomic, transcriptomic, and pharmacoepidemiologic study. PLoS Medicine, 2021, 18, e1003615.	8.4	38
47	An In Vivo Evaluation of Cerebral Cortical Amyloid with [18F]Flutemetamol Using Positron Emission Tomography Compared with Parietal Biopsy Samples in Living Normal Pressure Hydrocephalus Patients. Molecular Imaging and Biology, 2013, 15, 230-237.	2.6	36
48	Mu Opioid Receptor Binding Correlates with Nicotine Dependence and Reward in Smokers. PLoS ONE, 2014, 9, e113694.	2.5	36
49	Metabotropic glutamate receptor 5 tracer [18F]-FPEB displays increased binding potential in postcentral gyrus and cerebellum of male individuals with autism: a pilot PET study. Cerebellum and Ataxias, 2018, 5, 3.	1.9	36
50	The effect of ApoE ε4 on longitudinal brain region-specific glucose metabolism in patients with mild cognitive impairment: a FDG-PET study. NeuroImage: Clinical, 2019, 22, 101795.	2.7	34
51	Brain imaging research: Does the science serve clinical practice?. International Review of Psychiatry, 2007, 19, 541-558.	2.8	33
52	Risky decision-making and ventral striatal dopamine responses to amphetamine: A positron emission tomography [11C]raclopride study in healthy adults. NeuroImage, 2015, 113, 26-36.	4.2	29
53	The Competition Between Endogenous Dopamine and Radioligands for Specific Binding to Dopamine Receptors. Annals of the New York Academy of Sciences, 2002, 965, 440-450.	3.8	28
54	¹¹ C-MCG: Synthesis, Uptake Selectivity, and Primate PET of a Probe for Glutamate Carboxypeptidase II (NAALADase). Molecular Imaging, 2002, 1, 153535002002021.	1.4	27

#	Article	IF	CITATIONS
55	The distribution of the alpha7 nicotinic acetylcholine receptor in healthy aging: An in vivo positron emission tomography study with [18F]ASEM. NeuroImage, 2018, 165, 118-124.	4.2	27
56	Association of Intracranial Atherosclerotic Disease With Brain β-Amyloid Deposition. JAMA Neurology, 2020, 77, 350.	9.0	27
57	Brain imaging of cannabinoid type I (CB ₁) receptors in women with cannabis use disorder and male and female healthy controls. Addiction Biology, 2021, 26, e13061.	2.6	27
58	Effects of Substance Abuse on Ventricular and Sulcal Measures Assessed by Computerised Tomography. British Journal of Psychiatry, 1991, 159, 217-221.	2.8	26
59	Characterization of [11C]RO5013853, a novel PET tracer for the glycine transporter type 1 (GlyT1) in humans. NeuroImage, 2013, 75, 282-290.	4.2	26
60	Single photon emission computed tomography experience with (<i>S</i>)â€5â€{ ¹²³ l]iodoâ€3â€{2â€azetidinylmethoxy)pyridine in the living human brain of smoke and nonsmokers. Synapse, 2009, 63, 339-358.	er s 1.2	24
61	Feasibility Evaluation of Myocardial Cannabinoid Type 1 Receptor ImagingÂinÂObesity. JACC: Cardiovascular Imaging, 2018, 11, 320-332.	5.3	24
62	Model for reduced brain dopamine in Lesch-Nyhan syndrome and the mentally retarded: Neurobiology of neonatal-6-hydroxydopamine-lesioned rats. Mental Retardation and Developmental Disabilities Research Reviews, 1995, 1, 111-119.	3.6	23
63	Positron emission tomographic study of D2 dopamine receptor binding and CSF biogenic amine metabolites in rett syndrome. American Journal of Medical Genetics Part A, 1986, 25, 201-210.	2.4	22
64	High Availability of the α7-Nicotinic Acetylcholine Receptor in Brains of Individuals with Mild Cognitive Impairment: A Pilot Study Using ¹⁸ F-ASEM PET. Journal of Nuclear Medicine, 2020, 61, 423-426.	5.0	22
65	Doseâ€dependent, saturable occupancy of the metabotropic glutamate subtype 5 receptor by fenobam as measured with [¹¹ C]ABP688 PET imaging. Synapse, 2014, 68, 565-573.	1.2	21
66	The Association of Mid- and Late-Life Systemic Inflammation with Brain Amyloid Deposition: The ARIC-PET Study. Journal of Alzheimer's Disease, 2018, 66, 1041-1052.	2.6	20
67	Sex differences in the association between amyloid and longitudinal brain volume change in cognitively normal older adults. NeuroImage: Clinical, 2019, 22, 101769.	2.7	20
68	Generalizability of findings from a clinical sample to a communityâ€based sample: A comparison of ADNI and ARIC. Alzheimer's and Dementia, 2021, 17, 1265-1276.	0.8	20
69	In Vivo Imaging of D2 Dopamine Receptors in Schizophrenia. Archives of General Psychiatry, 2002, 59, 31.	12.3	19
70	Cerebral Expression of Metabotropic Glutamate Receptor Subtype 5 in Idiopathic Autism Spectrum Disorder and Fragile X Syndrome: A Pilot Study. International Journal of Molecular Sciences, 2021, 22, 2863.	4.1	19
71	Performance assessment of a NaI(Tl) gamma counter for PET applications with methods for improved quantitative accuracy and greater standardization. EJNMMI Physics, 2015, 2, .	2.7	18
72	Noncompartmental and compartmental modeling of the kinetics of carbon-11 labeled pyrilamine in the human brain. Synapse, 1993, 15, 263-275.	1.2	17

#	Article	IF	CITATIONS
73	Voltage-sensitive dye delivery through the blood brain barrier using adenosine receptor agonist regadenoson. Biomedical Optics Express, 2018, 9, 3915.	2.9	17
74	Pre-clinical characterization of [11C]R05013853 as a novel radiotracer for imaging of the glycine transporter type 1 by positron emission tomography. NeuroImage, 2013, 75, 291-300.	4.2	16
75	CSF Biomarkers and Its Associations with 18F-AV133 Cerebral VMAT2 Binding in Parkinson's Disease—A Preliminary Report. PLoS ONE, 2016, 11, e0164762.	2.5	16
76	Family history of alcoholism is related to increased D ₂ /D ₃ receptor binding potential: a marker of resilience or risk?. Addiction Biology, 2017, 22, 218-228.	2.6	15
77	Association between serotonin denervation and restingâ€state functional connectivity in mild cognitive impairment. Human Brain Mapping, 2017, 38, 3391-3401.	3.6	15
78	¹⁸ F-XTRA PET for Enhanced Imaging of the Extrathalamic α4β2 Nicotinic Acetylcholine Receptor. Journal of Nuclear Medicine, 2018, 59, 1603-1608.	5.0	15
79	β-amyloid deposition is associated with gait variability in usual aging. Gait and Posture, 2018, 61, 346-352.	1.4	15
80	Are dopamine receptor and transporter changes in Rett syndrome reflected in Mecp2-deficient mice?. Experimental Neurology, 2018, 307, 74-81.	4.1	15
81	Reduced Expression of Cerebral Metabotropic Glutamate Receptor Subtype 5 in Men with Fragile X Syndrome. Brain Sciences, 2020, 10, 899.	2.3	15
82	Beta-amyloid (Aβ) uptake by PET imaging in older HIV+ and HIV- individuals. Journal of NeuroVirology, 2020, 26, 382-390.	2.1	15
83	Radioligand binding analysis of α2 adrenoceptors with [11C]yohimbine in brain in vivo: Extended Inhibition Plot correction for plasma protein binding. Scientific Reports, 2017, 7, 15979.	3.3	14
84	Positron emission tomography–a tool for identifying the effects of alcohol dependence on the brain. Alcohol Research, 2003, 27, 161-73.	1.0	14
85	Quantification of [¹¹ C]yohimbine Binding to α ₂ Adrenoceptors in Rat Brain <i>in vivo</i> . Journal of Cerebral Blood Flow and Metabolism, 2015, 35, 501-511.	4.3	13
86	P4â€185: First inâ€human PET study of 3 novel tau radiopharmaceuticals: [¹¹ C]RO6924963, [¹¹ C]RO6931643, and [¹⁸ F]RO6958948. Alzheimer's and Dementia, 2015, 11, P850.	0.8	12
87	Effect of STN DBS on vesicular monoamine transporter 2 and glucose metabolism in Parkinson's disease. Parkinsonism and Related Disorders, 2019, 64, 235-241.	2.2	12
88	Imaging-based indices of Neuropathology and gait speed decline in older adults: the atherosclerosis risk in communities study. Brain Imaging and Behavior, 2021, 15, 2387-2396.	2.1	12
89	Effects of Vasopressin on Blood-Brain Transfer of Methionine in Dogs. Journal of Neurochemistry, 1992, 59, 1421-1429.	3.9	11
90	Voxelwise Relationships Between Distribution Volume Ratio and Cerebral Blood Flow: Implications for Analysis of β-Amyloid Images. Journal of Nuclear Medicine, 2015, 56, 1042-1047.	5.0	11

#	Article	IF	CITATIONS
91	Ethnic disparities in pain processing among healthy adults: μ-opioid receptor binding potential as a putative mechanism. Pain, 2020, 161, 810-820.	4.2	11
92	Neuronal insulin signaling and brain structure in nondemented older adults: the Atherosclerosis Risk in Communities Study. Neurobiology of Aging, 2021, 97, 65-72.	3.1	11
93	Brain opioid segments and striatal patterns of dopamine release induced by naloxone and morphine. Human Brain Mapping, 2022, 43, 1419-1430.	3.6	11
94	Association of Head Injury with Brain Amyloid Deposition: The ARIC-PET Study. Journal of Neurotrauma, 2019, 36, 2549-2557.	3.4	10
95	An open-label, positron emission tomography study of the striatal D2/D3 receptor occupancy and pharmacokinetics of single-dose oral brexpiprazole in healthy participants. European Journal of Clinical Pharmacology, 2021, 77, 717-725.	1.9	10
96	Cerebral Glucose Utilization in Polysubstance Abuse. Neuropsychopharmacology, 1995, 13, 21-31.	5.4	10
97	PET imaging of dopamine release in the frontal cortex of manganeseâ€exposed nonâ€human primates. Journal of Neurochemistry, 2019, 150, 188-201.	3.9	9
98	Cognitive Reserve in Midlife is not Associated with Amyloid-β Deposition in Late-Life. Journal of Alzheimer's Disease, 2019, 68, 517-521.	2.6	9
99	The association between midlife lipid levels and late-life brain amyloid deposition. Neurobiology of Aging, 2020, 92, 73-74.	3.1	9
100	Development of a radioligand for imaging V 1a vasopressin receptors with PET. European Journal of Medicinal Chemistry, 2017, 139, 644-656.	5.5	8
101	The Relationship of Varenicline Agonism of α4β2 Nicotinic Acetylcholine Receptors and Nicotine-Induced Dopamine Release in Nicotine-Dependent Humans. Nicotine and Tobacco Research, 2020, 22, 892-899.	2.6	8
102	Generalized dynamic PET inter-frame and intra-frame motion correction - Phantom and human validation studies. , 2012, , .		7
103	Synthesis and Evaluation of a New 18F-Labeled Radiotracer for Studying the GABAB Receptor in the Mouse Brain. ACS Chemical Neuroscience, 2018, 9, 1453-1461.	3.5	7
104	Fragile X Mental Retardation Protein and Cerebral Expression of Metabotropic Glutamate Receptor Subtype 5 in Men with Fragile X Syndrome: A Pilot Study. Brain Sciences, 2022, 12, 314.	2.3	7
105	In vivo studies of [125I]iodobenzamide and [11C]iodobenzamide: A ligand suitable for positron emission tomography imaging of cerebral D2 dopamine receptors. Synapse, 1992, 12, 236-241.	1.2	6
106	Direct 4D parametric image reconstruction with plasma input and reference tissue models in reversible binding imaging. , 2009, , .		6
107	ICâ€₽â€022: Conversion of Amyloid Quantitation With Florbetapir Suvr to The Centiloid Scale. Alzheimer's and Dementia, 2016, 12, P25.	0.8	6
108	Vestibular Function and Beta-Amyloid Deposition in the Baltimore Longitudinal Study of Aging. Frontiers in Aging Neuroscience, 2018, 10, 408.	3.4	6

#	Article	IF	CITATIONS
109	Deconvolution-based partial volume correction of PET images with parallel level set regularization. Physics in Medicine and Biology, 2021, 66, 145003.	3.0	6
110	Imaging in drug discovery, preclinical, and early clinical development. Journal of Nuclear Medicine, 2008, 49, 26N-28N.	5.0	6
111	Direct 4D reconstruction of parametric images incorporating anato-functional joint entropy. , 2008, , .		5
112	Generalized inter-frame and intra-frame motion correction in PET imaging - a simulation study. , 2011, , .		5
113	A three-step reconstruction method for fluorescence molecular tomography based on compressive sensing. , 2017, 10059, .		5
114	Density of available striatal dopamine receptors predicts trait impulsiveness during performance of an attention-demanding task. Journal of Neurophysiology, 2017, 118, 64-68.	1.8	5
115	[ICâ€Pâ€188]: ON EVALUATION OF TAU ACCUMULATIONS IN LONGITUDINAL STUDIES OF ALZHEIMER'S DISEASE (AD): IMPLICATIONS FROM A PET STUDY WITH [18F]RO6958948. Alzheimer's and Dementia, 2017, 13, P139.	0.8	5
116	Image reconstruction in fluorescence molecular tomography with sparsity-initialized maximum-likelihood expectation maximization. Biomedical Optics Express, 2018, 9, 3106.	2.9	5
117	A cholecystokinin B receptor antagonist and cocaine interaction, phase I study. CNS Neuroscience and Therapeutics, 2019, 25, 136-146.	3.9	5
118	Dataset of quantitative structured office measurements of movements in the extremities. Data in Brief, 2020, 31, 105876.	1.0	5
119	The prospective association between periodontal disease and brain imaging outcomes: The Atherosclerosis Risk in Communities study. Journal of Clinical Periodontology, 2022, 49, 322-334.	4.9	5
120	Deformation field correction for spatial normalization of PET images. NeuroImage, 2015, 119, 152-163.	4.2	4
121	Mid- and Late-Life Leisure-Time Physical Activity and Global Brain Amyloid Burden: The Atherosclerosis Risk in Communities (ARIC)-PET Study. Journal of Alzheimer's Disease, 2020, 76, 139-147.	2.6	4
122	Is getting older all that rewarding?. Proceedings of the National Academy of Sciences of the United States of America, 2008, 105, 14751-14752.	7.1	3
123	Incorporating reflection boundary conditions in the Neumann series radiative transport equation: application to photon propagation and reconstruction in diffuse optical imaging. Biomedical Optics Express, 2018, 9, 1389.	2.9	3
124	Association of PET-measured myocardial flow reserve with echocardiography-estimated pulmonary artery systolic pressure in patients with hypertrophic cardiomyopathy. PLoS ONE, 2019, 14, e0212573.	2.5	3
125	Relative strengths of three linearizations of receptor availability: Saturation, Inhibition, and Occupancy plots. Journal of Nuclear Medicine, 2021, , jnumed.117.204453.	5.0	3
126	Phase 1 Evaluation of C-CS1P1 to Assess Safety and Dosimetry in Human Participants Journal of Nuclear Medicine, 2022, , .	5.0	3

#	Article	IF	CITATIONS
127	A radiative transfer equation-based image-reconstruction method incorporating boundary conditions for diffuse optical imaging. , 2017, 10137, .		2
128	Characterization of dose dependent norepinephrine transporter blockade by atomoxetine in human brain using 11C MeNER PET. Journal of Cerebral Blood Flow and Metabolism, 2005, 25, S599-S599.	4.3	2
129	Spectral analysis with a minimal basis functions approach for quantification of ligand-receptor dynamic PET study. Journal of Cerebral Blood Flow and Metabolism, 2005, 25, S634-S634.	4.3	2
130	Brain Imaging Features Associated with 20-Year Cognitive Decline in a Community-Based Multiethnic Cohort without Dementia. Neuroepidemiology, 2022, 56, 183-191.	2.3	2
131	P4-187: Midlife adiposity predicts earlier onset of Alzheimer's dementia, neuropathology, and presymptomatic cerebral amyloid accumulation. , 2015, 11, P851-P852.		1
132	Data Processing Methods for a High Throughput Brain Imaging PET Research Center. , 2006, , .		0
133	Motion-incorporated partial volume correction: Methodology and validation. , 2010, , .		0
134	P4-186: Kinetic evaluation of three newly developed radioligands for human tau imaging. , 2015, 11, P851-P851.		0
135	IC-P-125: Arterial Stiffness and β-Amyloid Deposition in The ARIC-PET Study. , 2016, 12, P93-P93.		0
136	P3-242: Conversion of Amyloid Quantitation with Florbetapir SUVR to the Centiloid Scale. , 2016, 12, P919-P920.		0
137	Notice of Removal: Real-time recording of neuronal voltage membrane variation during seizure using transcranial photoacoustic voltage-sensitive dye imaging. , 2017, , .		0
138	P3â€423: INDEPENDENT AND SYNERGISTIC EFFECTS OF AMYLOID PATHOLOGY AND HIPPOCAMPAL NEURODEGENERATION ON COGNITIVE CHANGE IN COGNITIVELY NORMAL OLDER ADULTS. Alzheimer's and Dementia, 2018, 14, P1271.	0.8	0
139	Remission of Gilles de la Tourette Syndrome after Heat-Induced Dehydration. International Journal of Physical Medicine & Rehabilitation, 2018, 06, .	0.5	0
140	ICâ€₽â€001: SURROGATES OF REGIONAL CEREBRAL BLOOD FLOW COMPUTED FROM DYNAMIC AMYLOID PET IMAGING. Alzheimer's and Dementia, 2018, 14, P14.	0.8	0
141	Learning Mechanisms Underlying Value-Driven Attention. Journal of Vision, 2017, 17, 1101.	0.3	0
142	Medial Temporal Tau Pathology Is Associated With Verbal Memory. Innovation in Aging, 2020, 4, 767-767.	0.1	0
143	Associations Between Atrial Arrhythmias and Brain Amyloid Deposition: The ARIC-PET Study. Journal of Alzheimer's Disease, 2022, 86, 43-48.	2.6	0
144	Age of amyloid onset, but not amyloid accumulation rate, differs across APOEâ€e4 carriers vs. nonâ€earriers in three cohorts and three methods. Alzheimer's and Dementia, 2021, 17, .	0.8	0

#	Article	IF	CITATIONS
145	Carotid Intima-Media Thickness and Amyloid-β Deposition: The ARIC-PET Study. Journal of Alzheimer's Disease, 2022, , 1-6.	2.6	Ο